Microporous and Mesoporous Materials 162 (2012) 181–188

Contents lists available at SciVerse ScienceDirect

Microporous and Mesoporous Materials

journal homepage: www.elsevier.com/locate/micromeso

# Effect of surfactants on the porogen size in the low-*k* methylsilsesquioxane/polystyrene hybrid films

Yu-Han Chen, Hung-En Tu, Jihperng Leu *

*Department of Materials Science and Engineering, National Chiao Tung University, No.1001, University Road, Hsinchu 30010, Taiwan*

ARTICLE INFO

*Article history:*
Received 23 March 2012
Received in revised form 20 May 2012
Accepted 24 May 2012
Available online 21 June 2012

*Keywords:*
Porogen
Pore size
Surfactant
Low-*k*
GISAXS

ABSTRACT

An anionic surfactant, sodium dodecylbenzenesulfonate (NaDBS) and a cationic surfactant, domiphen bromide (DB) were used to modify the surface potential of polystyrene (PS) porogen in a post-integration porogen removal scheme. The effect of surfactant modification on the porogen and pore size in the low-*k* methylsilsesquioxane (MSQ)/PS hybrid films at 10 wt% PS loading, under a slow curing rate, was studied by grazing incidence small-angle X-ray scattering, viscosity measurement, and Fourier-transform infrared analysis. For PS porogen without modification, the porogen aggregated and its size increased from 10.0 to 16.5 nm at different rates, up to 200 °C, depending on the porogen diffusivity and steric hindrance by the successively cross-linked MSQ matrix at $T \geqslant T_g$. In contrast, the NaDBS- and DB-modified porogens with higher surface potential impede their aggregation within the cross-linking MSQ matrix, resulting in a smaller porogen size, by electrostatic repulsion and increased viscosity due to electroviscous effect. Also, the columbic attraction between Si−OH groups of MSQ matrix and the positively charged, DB-modified PS, restrains the PS porogen, thus reduces its aggregation during cure step, leading to a small porogen size and tight distribution (8.7 ± 2 nm) at 200 °C and later a similar pore size after porogen removal at 400 °C.



## 1. Introduction

As device scaling developed beyond the 0.18 μm node, RC delay in the backend interconnect became an obstacle [1]. In order to alleviate this problem, low dielectric constant (low-*k*) materials ($k = 2.5–3.2$) such as carbon-doped oxide or SiLK™ were introduced after the copper interconnect was first implemented [2,3]. Moving further toward the 22 nm node and beyond, the incorporation of porosity, in which air has $k_{air} = 1$, becomes essential for producing viable low-*k* materials with $k < 2.5$ [4]. Conventionally, porous low-*k* dielectric films are generally formed by depositing a low-*k* matrix with a thermally liable pore generator (porogen) [5], which is burned out by thermal treatment at low temperatures, typically ⩽200 °C immediately after film deposition. However, such porous films suffer from reliability issues, such as high leakage and low dielectric breakdown strength at the barrier/low-*k* interface, because of the insufficient coverage for large pores caused by plasma damage during the etching process [6–8]. To circumvent such reliability issues, a novel post-integration porogen removal method is proposed, which uses a high decomposition temperature (>350 °C) porogen in the material design and an integration scheme [7–10]. It uses a high-temperature porogen, such as poly(styrene-b-butadiene-b-styrene), and poly(styrene-b-4-vinylpyridine) [11] to defer the formation of a porous low-*k* dielectric, until the completion of the copper chemical mechanical polishing (CMP) step, and then thermally removes the sacrificial porogen from the hybrid dielectric film. In this case, the aggregation of porogen and the interaction between porogen and the low-*k* matrix during curing may significantly affect the porogen size and distribution of low-*k*/porogen hybrid films, which, in turn, influence the low-*k* film's mechanical properties [12] and barrier reliability upon the removal of porogens. Several approaches have been undertaken to improve the porogen size and distribution in hybrid low-*k* materials. The curing temperature and ramp rate have been used to reduce the porogen size in low-*k* hybrid materials through the retardation of porogen segregation by the rate of matrix cross-linking [13,14]. A fast curing rate can achieve smaller porogen size and tighter distribution by rapidly forming a cross-linked low-*k* matrix to freeze up porogen aggregation sterically [13]. Still, there is a strong need for versatile curing processes such as slow ramp rate, for tailoring specific properties, for example, a lower film stress for better film integrity [15,16]. Yet, the dispersion of porogen and its impact on the aggregation behavior of porogens prior to the formation of a cross-linked low-*k* matrix has not been fully explored and understood. A huge amount of research concerning particle dispersion in colloids shows that the state of the dispersion can be modified, for example, by a highly charged, sterically

* Corresponding author. Tel.: +886 3 571 2121/31420; fax: +886 3 572 4727.
*E-mail address:* jimleu@mail.nctu.edu.tw (J. Leu).

1387-1811/$ - see front matter © 2012 Elsevier Inc. All rights reserved.
http://dx.doi.org/10.1016/j.micromeso.2012.05.042

stabilized polymer and pH value to obtain a high-stability dispersion with the electrostatic and steric effect [17–19]. Thus, this study explores the electrostatic and steric dispersion of polymer porogens within a low-*k* matrix to control the porogen size in low-*k* hybrid films at a slow cure rate.

This study uses a commercial, spin-on organosilicate, methylsilsesquioxane (MSQ), as the matrix and polystyrene (PS) as a porogen in a novel post-integration porogen removal method for preparing porous low-*k* MSQ film. An anionic surfactant, sodium dodecylbenzenesulfonate (NaDBS) and a cationic surfactant, domiphen bromide (DB), were used to modify the PS surface in the solution and the MSQ/PS hybrid films. The effect of surfactant modification on the porogen and pore size in the low-*k* methylsilsesquioxane (MSQ)/PS hybrid films at 10 wt% PS loading, under a slow curing rate, was studied by grazing incidence small-angle X-ray scattering (GISAXS), viscosity measurement, and Fourier-transform infrared (FTIR) analysis. The mechanism for determining the PS porogen aggregation with and without surfactant modification, as well as the porogen size and pore size, within a successively crosslinked MSQ matrix will be described and elucidated.

## 2. Experimental

The low-*k* matrix, MSQ, was obtained from Gelest Inc. PS ($M_w$ = 790 g/mole), the high temperature porogen, was obtained from Sigma–Aldrich Co. NaDBS ($M_w$ = 348.48 g/mole), an anionic surfactant, was procured from Showa Chemical Industry Co., Ltd. DB ($M_w$ = 414.48 g/mole), and a cationic surfactant, was obtained from Sigma–Aldrich Co. PS particles were first dissolved in tetrahydrofuran (THF) to form a solution without modification (pH ~7.0). In addition, pH value and surfactants were used to modify the surface property of the PS particles. For pH effect, PS solutions with pH values of 3 and 11 were prepared by adding acid and base, respectively. Moreover, the well-dispersed PS/THF solutions were modified by two types of surfactants: (1) anionic surfactant, NaDBS, below its critical micelle concentration (CMC) of 522.75 mg/L, and (2) cationic surfactant, DB below its CMC of 730.74 mg/L [20]. The zeta potentials of the PS/THF solutions with and without modification were measured using a Zeta Potential Analyzer (Zetasizer HSA3000, Malvern Instruments). The size of the PS particles in the THF solution was measured using an Ultrafine Particle Analyzer (Honeywell UPA 150).

Then, MSQ and PS particles (with and without surface modification) at 10 wt% loading were dissolved in THF solvent to form a hybrid low-*k* solution. The solution was initially filtered through a 0.20 μm PTFE filter (Millipore Inc.), and then spun onto a (100) silicon wafer at 2000 rpm for 30 s at room temperature to obtain a film thickness of 500 nm. The size and distribution of the porogen in the hybrid low-*k* films during the curing step at 2 °C/min were then characterized by *in situ* GISAXS using Beamline 23A of the National Synchrotron Radiation Research Center (NSRRC), Hsinchu, Taiwan. *In situ* 2D GISAXS data were collected from 30 to 200 °C at intervals of 10 °C. All of the GISAXS data were obtained using an area detector covering a $q$ range from 0.01 to 0.1 $Å^{-1}$, and the incident angle of the X-ray beam (0.5 mm diameter) was fixed at 0.2° with an X-ray energy of 10 keV. Then, the porogen size was analyzed using sphere-model fitting and Guinier's law [21,22].

The interaction between MSQ and PS was then examined by an *in situ* viscosity measurement using ARES (Rheometric Scientific). The viscosity data were collected from room temperature to 200 °C for the MSQ/PS hybrid films with and without modification by surfactants. The interaction between MSQ and surfactant-modified PS was further investigated using a FTIR spectrometer, MAGNA-IR 460 (Nicolet Inc.) in a transmission mode with 64 scans at a spectral resolution of 2 $cm^{-1}$.

Finally, the hybrid films (with and without modification) were cured in a quartz tube furnace under $N_2$ at a heating rate of 2 °C/min to 400 °C for 1 h to form the porous low-*k* films after completely burning out the porogens. Their pore sizes were also characterized using the GISAXS technique. The porosity of the porous low-*k* films were obtained from its density, which was measured by X-ray reflectivity (XRR) (Bruker D8 Discover), with a Cu $K_\alpha$ source ($\lambda$ = 0.154 nm), using $\omega$-2$\theta$ scan mode. The scanning region ranged from 0° to 2°. The XRR data was analyzed by LEPTOS simulation software, to fit the density of porous low-*k* film.

## 3. Results and discussion

Zeta potential has been recognized as a measure of the magnitude of the repulsion or attraction between particles in colloids [23]. Such measurement provides an insight into the dispersion of PS porogens in THF solvent. This helps us to understand how the porogen size in the solution is affected by the electrostatic dispersion due to surface modification of the PS. Table 1 summarizes the zeta potential and the corresponding particle size of PS porogen in the THF solution as a function of surface modification. The particle sizes of the PS in the solution were measured to be 12.3 ± 2.5, 49.3 ± 4.1 and 11.2 ± 2.4 nm for PS/THF solutions at a pH value of 3, 7 (as-prepared without modification), and 11, respectively. And the corresponding zeta potentials of the PS/THF solution were +28, −18, and −40 mV. This indicates that a higher absolute surface potential led to a smaller PS particle size. The relationship between zeta potential and PS particle size can be described by Eq. (1) [24].

$$\zeta = \frac{q}{4\pi\varepsilon r} \tag{1}$$

where $\zeta$ is the zeta potential of the particle, $q$ is the electronic charge, $\varepsilon$ is the dielectric constant of the particle, and $r$ is the radius of the particle. Our finding on the effect of pH values is consistent with an earlier report that the larger absolute value of potential (>25 mV) results in better colloidal stability and a smaller particle size, due to electrostatic dispersion [24]. In addition, Table 1 shows that the particle sizes of PS in the solution modified by anionic and cationic surfactants, were further reduced to 9.0 ± 2.0 nm and 8.0 ± 1.8 nm because of their relatively higher, absolute surface potential of −58 and +66 mV, respectively.

Based on the particle size data, we will focus on the modification of PS by anionic and cationic surfactant for producing low-*k* MSQ/PS hybrid film and the corresponding porous low-*k* film in this study. More specifically, MSQ matrix precursor was added to PS/THF solutions with and without surfactant modification. Subsequently, the solutions were spin-coated onto silicon wafer to fabricate the as-prepared low-*k* hybrid films. The sizes of PS porogens in the hybrid low-*k* films, cured at a slow rate, i.e. 2 °C/min from 30 to 200 °C, was then *in situ* characterized by 2D GISAXS. Fig. 1a–c show the GISAXS patterns of the low-*k* PS/MSQ hybrid films at representative temperatures from 30 to 190 °C (40 °C intervals) for PS porogens without and with NaDBS and DB surfactant modification, respectively. With increasing temperature, scattering patterns illustrated in Fig. 1a, were confined in the low-$q$ region, indicating

**Table 1**
The zeta potential and the corresponding particle size of PS porogen in the solution as a function of surface modification.

| Treatment on PS | Zeta potential (mV) | PS particle size (nm) |
|---|---|---|
| No modification | −18 | 49.3 ± 4.1 |
| pH = 3 | +28 | 12.3 ± 2.5 |
| pH = 11 | −40 | 11.2 ± 2.4 |
| Anionic surfactant NaDBS | −58 | 9.0 ± 2.0 |
| Cationic surfactant DB | +66 | 8.0 ± 1.8 |

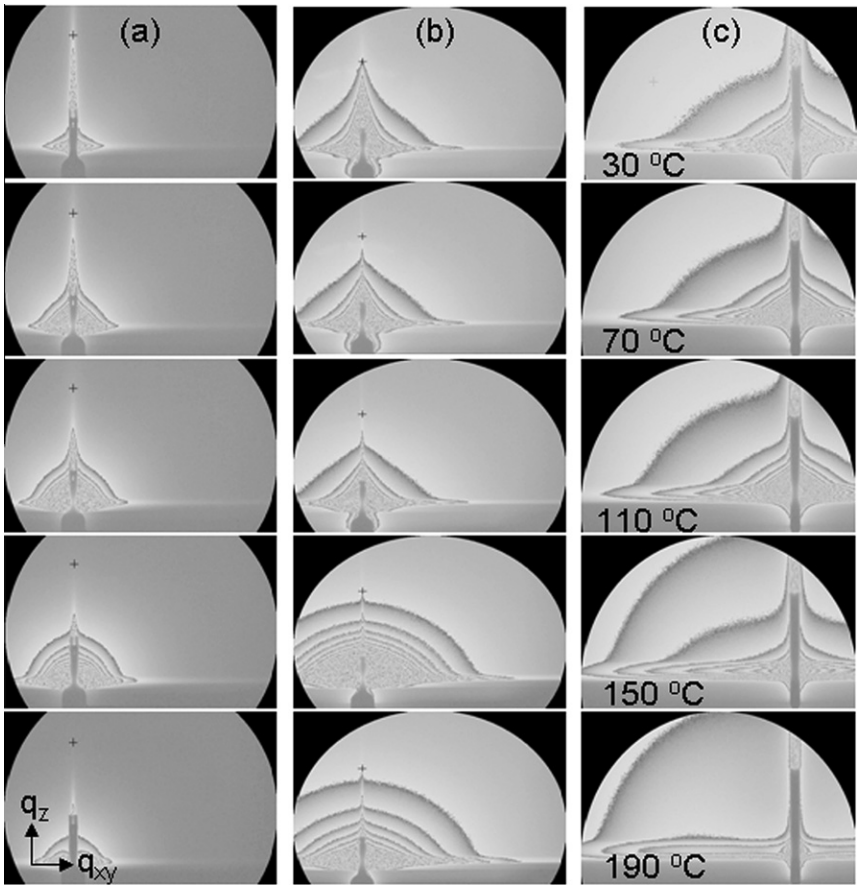


**Fig. 1.** 2-D GISAXS scattering patterns of the low-*k* MSQ/PS hybrid films as a function of cure temperature: (a) PS without modification, (b) NaDBS-modified PS, and (c) DB-modified PS.

that the PS porogens tended to aggregate and did not disperse well in the low-*k* PS/MSQ hybrid film. In contrast, the scattering patterns shown in Fig. 1b (NaDBS) and c (DB) were stronger and more uniform in the high-*q* region than the corresponding ones without surface modification (Fig. 1a). The results of these successive scattering patterns indicates that the porogen size in the modified low-*k* hybrid films was smaller than that of the unmodified films at the same cure temperatures.

In order to compare the effect of surfactant treatment on the porogen size and its evolution during the curing step, the PS porogen size/distribution was quantitatively determined by the same method described in detail elsewhere [13]. Accordingly, the calculated porogen size and distribution of the hybrid low-*k* films with and without NaDBS and DB modification, as a function of curing temperatures are shown in Fig. 2a, b and c, respectively. For low-*k* hybrid film without modification shown in Fig. 2a, the porogen size/distribution increased noticeably from 10.0 ± 2.4 nm to 16.5 ± 5.5 nm from 30 to 190 °C. Moreover, the increased rate of porogen size became noticeable at $T \geqslant 110$ °C, and more significant between 130 and 170 °C (from 11.4 ± 3.9 nm to 15.6 ± 4.9 nm), but less between 170 and 190 °C (from 15.6 ± 4.9 nm to 16.5 ± 5.5 nm). In the NaDBS modification case (Fig. 2b), the porogen size and distribution increased slightly and linearly from 9.0 ± 2.0 nm at 30 °C to 11.1 ± 2.4 nm at 190 °C. In contrast, for PS modified by DB (Fig. 2c), the porogen size and distribution changed only slightly from 7.8 ± 1.0 nm at 30 °C to 8.7 ± 2.0 nm at 190 °C. Overall, modification of PS porogen by cationic surfactant, DB yielded the smallest porogen size and tightest distribution.

Next, we examine the pore size in the porous low-*k* MSQ films after removing the PS porogens in the above-mentioned 3 different MSQ/PS hybrid films at 400 °C. Fig. 3a–c show the GISAXS patterns of the porous low-*k* MSQ films prepared from the unmodified PS, NaDBS-modified PS, and DB-modified PS system, respectively. The stronger scattering intensities in Fig. 3b and c indicate smaller and uniform pores in the porous films prepared from surfactant-modified PS porogens. Specifically, the pore sizes were calculated to be 16.8, 11.5, and 8.8 nm for these 3 different systems. In addition, the porosity of the porous low-*k* film at 10 wt% PS loading was found to be 15.6% by using the XRR technique. Compared to the porogen size in the hybrid films cured at 190 °C, there was little aggregation of PS porogens once MSQ was fully cross-linked at 200 °C.

Based on particle analysis of the PS/THF solution and *in situ* GISAXS analysis of the low-*k* MSQ/PS hybrid films, the PS size in the solution and the hybrid film, then the pore size after burn-out, can be summarized below. The PS particles in the THF solvent without modification could diffuse and aggregate readily into large particles with a size of 49.3 nm. When MSQ precursor was added to the solution to form a low-*k* hybrid film, the PS porogen size was found to be 10.0 nm at 30 °C. These results indicate that PS particles without surfactant treatment were shrunk by the presence of MSQ matrix precursor in the hybrid film due to the steric effect [25,26]. In contrast, the PS with NaDBS and DB modification in the solution showed a much smaller particle size of 9.0 and 8.0 nm, respectively. The difference can be attributed to the electrostatic dispersion due to their higher absolute zeta potentials as described in the previous section. When MSQ precursor was added to the PS/THF solution with NaDBS and DB modification, then spin-coated to form a low-*k* hybrid film, the PS porogen size remained at 9.0 and 7.8 nm at 30 °C, respectively. This indicates that the electrostatic

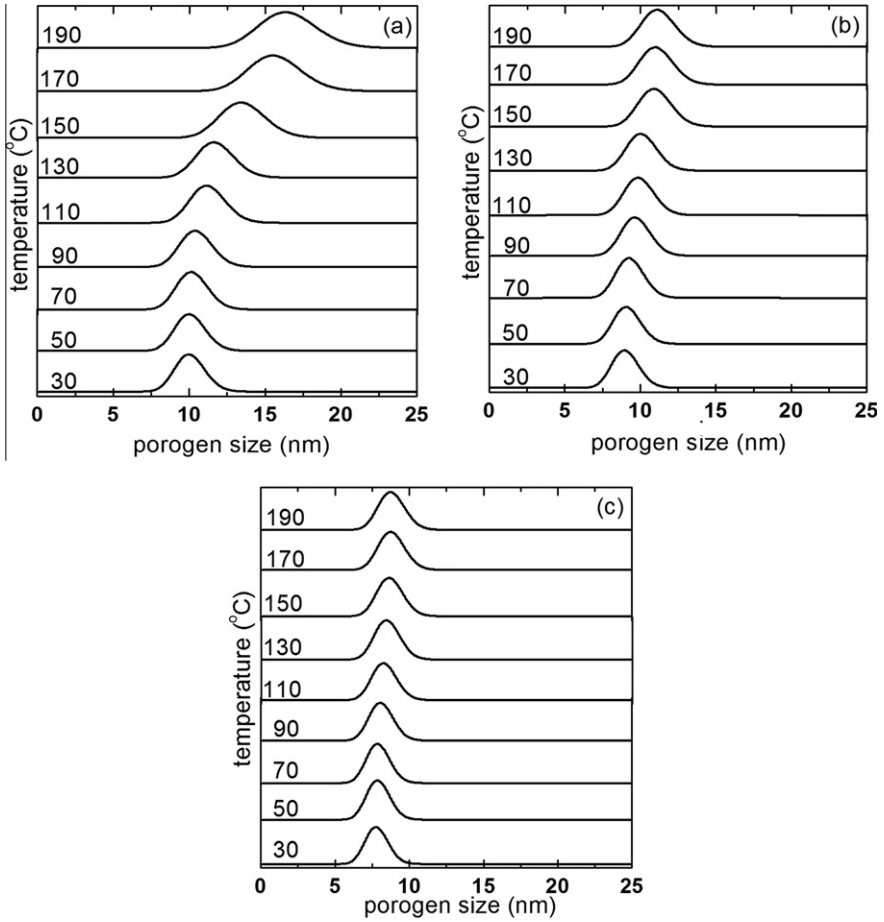


**Fig. 2.** Porogen sizes and distribution in the low-*k* MSQ/PS hybrid films as a function of cure temperature: (a) PS without modification, (b) NaDBS-modified PS, and (c) DB-modified PS.

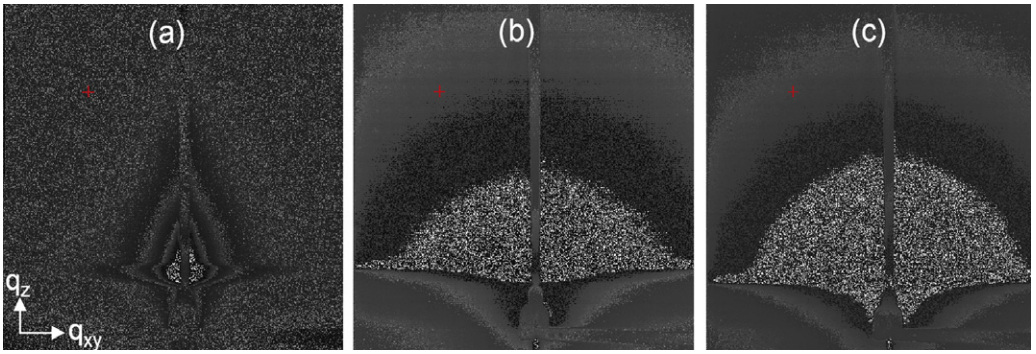


**Fig. 3.** 2-D GISAXS scattering patterns of the low-*k* porous MSQ films after removal of PS porogens at 400 °C: (a) PS without modification, (b) NaDBS-modified PS, and (c) DB-modified PS.

dispersion effect by surfactant was dominant over the steric effect by MSQ matrix.

When the low-*k* hybrid films were further cured to 190 °C, the porogen size was increased by 23.3% from 9.0 to 11.1 nm for the NaDBS-modified PS system; and increased by 11.5% from 7.8 to 8.7 nm for the DB-modified PS system, but increased significantly, by 65.0% from 10.0 to 16.5 nm for the system without modification. After the removal of PS porogens at 400 °C, the pore sizes were about the same as those at cured at 200 °C, showing that there was little aggregation of PS porogens once MSQ was fully cross-linked at 200 °C. Thus, surfactant modification of PS, especially by DB, can achieve and maintain a small pore size with tight distribution, even at a slow cure rate, i.e. 2 °C/min. Thus, the porogen aggregation behavior within the cross-linkable MSQ matrix as a function of cure temperature up to 200 °C is critical for controlling the porogen and pore size after burn-out. This will be addressed in the following sections.

*In situ* viscosity measurement was carried out from room temperature to 200 °C to examine any aggregation of porogens and the interaction between porogens and progressively cross-linked MSQ. In addition, the cross-linking behavior of MSQ in the low-*k* MSQ/PS hybrid films was investigated by FTIR analysis. The viscos-

ity, porogen size, and network/cage structure ratio of the MSQ/PS hybrid films with and without modification, as a function of temperature at a heating rate of 2 °C/min from 30 to 200 °C, are shown in Fig. 4a, b, and c, respectively. In the unmodified case, porogen size did not change much at $T < 100$ °C. Then, the viscosity reached a plateau and remained at $\sim 2.3 \times 10^5$ poises between 105 and 160 °C (Fig. 4a). The porogen size noticeably increased by 15% (relative to the size at 30 °C) at 130 °C and 33% at 150 °C (Fig. 4b). As the cure temperature was further increased, the viscosity would drop at the on-set temperature of about 160 °C and reached its lowest value, $\sim 1.8 \times 10^5$ poises at 175 °C (Fig. 4a), while the porogen size was enlarged by 50% at 170 °C (Fig. 4b). In the last stage up to 190 °C, the porogen size increased by 65%. But, the rate of size change was reduced because MSQ was almost entirely cross-linked as illustrated by the network/cage ratio (Fig. 4c).

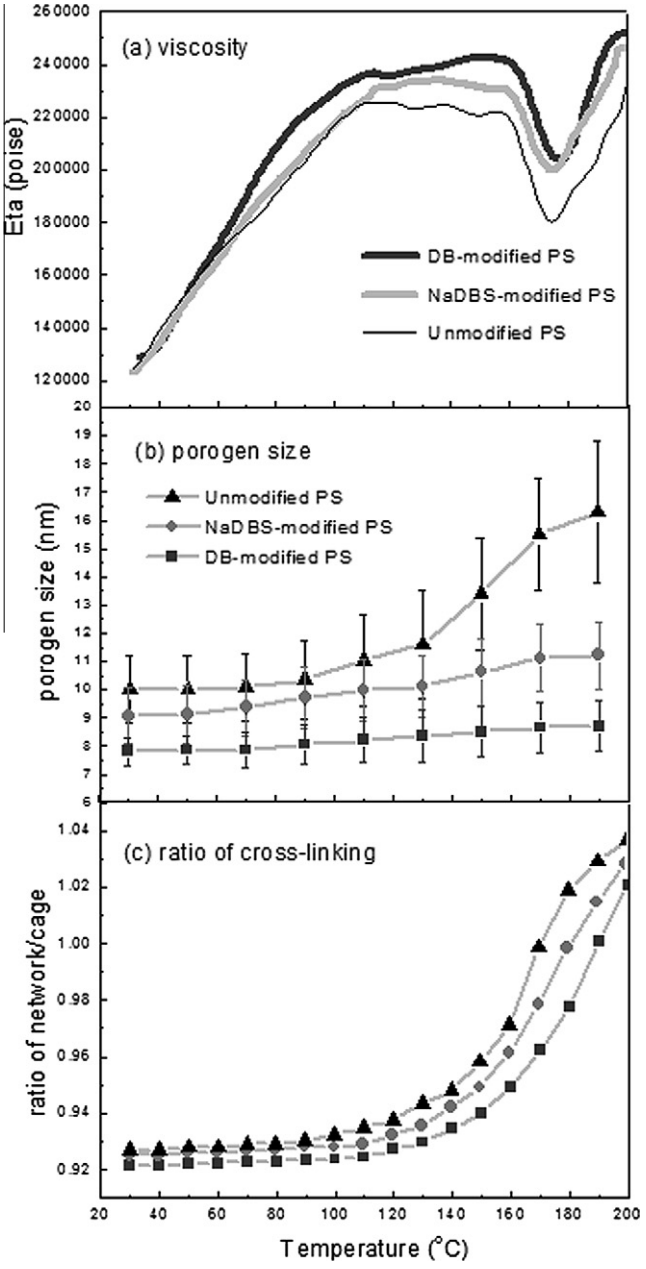


**Fig. 4.** (a) The viscosity, (b) porogen size, and (c) the ratio of network-/cage- Si–O in the low-$k$ MSQ/PS hybrid films as a function of cure temperature for NaDBS-modified PS (●), DB-modified PS (■), and PS without modification (▲).

The results indicate that the PS porogen without treatment can diffuse and aggregate readily in the relaxed MSQ structure at $T_g \leqslant T \leqslant 160$ °C. The aggregation was enhanced at $T > 160$ °C due to viscosity reduction by $H_2O$ released from the on-set of condensation, i.e. cross-linking of the MSQ matrix, resulting in an increase in porogen size at a faster rate. At $T > 175$ °C, viscosity increased again as the cross-linking of the MSQ matrix was near completion, leading to a continued increase in porogen size to 16.5 nm at 200 °C, but a lower rate.

In the NaDBS-modified PS case, Fig. 4b shows that the PS porogen size increases very little from 9.0 nm at 30 °C to ~10 nm at 150 °C, then to 11.0 nm at $T > 170$ °C. Interestingly, it exhibits higher viscosity ($\sim 2.3 \times 10^5$ poises) than the hybrid film without modification ($\sim 2.2 \times 10^5$ poises) in the 105–160 °C range as shown in Fig. 4a. While the on-set temperatures for the viscosity drop (160 °C) and viscosity pickup (175 °C) for both systems are the same, the viscosity of the NaDBS-modified hybrid film remained higher, $\sim 2.3 \times 10^5$ poises at 160 °C and $\sim 2.0 \times 10^5$ poises (vs. $\sim 1.8 \times 10^5$ poises for the unmodified system) at 175 °C. The degree of cross-linking of the MSQ matrix in the NaDBS-modified MSQ/PS hybrid system (Fig. 4c) was slightly lower than the unmodified system, presumably due to its higher viscosity. Nevertheless, this indicates that the addition of anionic surfactant does not noticeably affect the cross-linking behavior of MSQ. This is confirmed by the same on-set temperatures of viscosity drop at 160 °C and the rapid rise in viscosity at ~175 °C as shown in Fig. 4a.

In the cationic DB-modified PS system, Fig. 4b shows that the PS porogen size increases very little from 7.8 nm at 30 °C to ~8.7 nm at $T > 170$ °C. This system exhibited higher viscosity (max. $\sim 2.4 \times 10^5$ poises) than the hybrid film without modification (max. $\sim 2.2 \times 10^5$ poises) and even the NaDBS-modified hybrid film (max. $\sim 2.3 \times 10^5$ poises) throughout the whole temperature range. Moreover, its viscosity did not show an obvious plateau prior to the on-set condensation temperature, i.e. at $T_g \leqslant T \leqslant 160$ °C. However, the viscosity curve shows that the on-set temperature of viscosity drop in the DB-modified PS system was delayed by about 5 °C, compared to the other two conditions. Also, the degree of cross-linking of the MSQ matrix in the DB-modified PS system (Fig. 4c) was the lowest. This shows that the addition of cationic surfactant does noticeably affect the cross-linking behavior of MSQ in the hybrid film during the curing step.

The interaction between MSQ and surfactant-modified PS was then further investigated by monitoring changes in the of Si–OH infrared absorption band in the 905–930 $cm^{-1}$ region of the MSQ/PS hybrid films at room temperature by FTIR spectroscopy. Fig. 5 shows a cage Si–O structure at ~1130 $cm^{-1}$ and a network Si–O structure at ~1030 $cm^{-1}$ [27], and a Si–OH stretching band in the 905–930 $cm^{-1}$ region [28,29]. In particular, the peak positions of Si–OH of MSQ for the unmodified, NaDBS-, and DB-modified PS systems were 922, 924, and 908 $cm^{-1}$, respectively. Compared to the unmodified and anionic surfactant-modified PS systems with a negative surface potential, the strong red shift, 14 $cm^{-1}$ in the Si–OH band for the cationic DB-modified PS system can be attributed to columbic attraction [30] between the electron lone pair of oxygen atoms of the Si–OH group and the positively charged PS particles (with a surface potential of +66 mV).

The next task is to clarify whether the attractive force between the Si–OH and DB-modified PS porogen affects the MSQ matrix cross-linking and porogen aggregation during the curing step. Therefore, the peak positions and peak intensities of the Si–OH absorption band of MSQ with and without modification, as a function of cure temperature are further examined and illustrated in Fig. 6a and b, respectively. Fig. 6a shows that the peak positions of Si–OH in the negatively charged PS system remained at ~922 $cm^{-1}$ without any obvious change at $T \leqslant 140$ °C. This implies that the electrostatic force between charged PS and MSQ is not af-

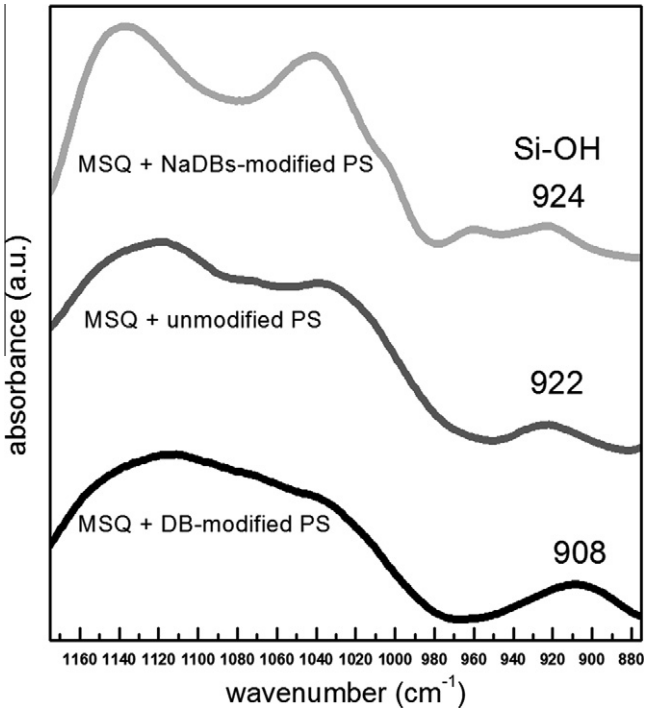


**Fig. 5.** FTIR spectra (880 to 1170 $cm^{-1}$) of low-*k* MSQ/PS hybrid films at 25 °C for PS without modification, NaDBS-modified, and DB-modified PS.

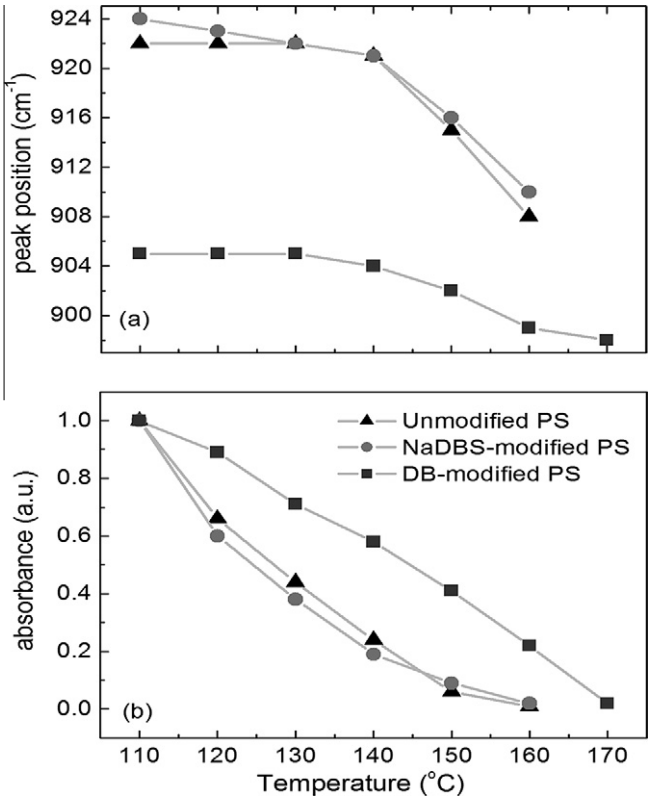


**Fig. 6.** (a) Peak position and (b) peak intensity of Si–OH infrared absorption band as a function of cure temperature for NaDBS-modified PS (●), DB-modified PS (■), and PS without modification (▲).

fected by cure temperature below 140 °C. The peak position then shifted noticeably to 908 $cm^{-1}$ at temperatures between 140 °C and 160 °C. This can be attributed to the hydrogen bonding interaction [31] as Si–OH groups come in a closer range due to a drop of viscosity, and start a condensation reaction at this stage. Similarly, the peak position of the positively charged, DB-modified PS system remained at 905 $cm^{-1}$ until 150 °C, then shifted gradually to 898 $cm^{-1}$ due to the cross-linking of MSQ. The Si–OH band was still present at 170 °C, which is about 10 °C offset compared to the negatively charged and unmodified PS systems.

Fig. 6b shows that the intensity of the Si–OH peak decreases with increasing cure temperatures of >100 °C, except that the rate of change is much slower for the DB-modified PS system. The decrease in the Si–OH band intensity was due to the condensation of Si–OH groups in the MSQ precursor, leading to a cross-linked, cage to network Si–O structure [32]. Thus, the cross-linking rate in the positively charged, DB-modified system was slower than those in the negatively charged PS systems (without modification or NaDBS-modified) presumably due to the columbic attractive force between Si–OH and positively charged PS porogens, as evidenced by the red-shift in the Si–OH band (Fig. 5).

Based on the FTIR results, the interaction mechanism between the MSQ matrix and surfactant-modified PS porogen, especially the positively charged, DB-modified PS can be elucidated. Its correlation with the degree of cross-linking, the viscosity, and the porogen size in the hybrid films prepared at a slow cure rate, using GISAXS, FTIR and viscosity measurements, is also clarified. The aggregation of the PS porogen in the low-*k* hybrid PS/MSQ films is greatly influenced by electrostatic stabilization [33], steric stabilization of cross-linkable MSQ matrix, and interaction between the MSQ matrix and surface-modified PS, depending on the zeta potential and charge state of surfactants.

As our previous work on MSQ/polystyrene-b-polybutadiene-b-polystyrene (SBS) porogen [13], the steric barrier effect on the PS porogens is affected by the microstructure of the cross-linkable MSQ matrix at three significant temperatures in the cure step; namely, (1) the glass transition temperature, $T_g$ (~100 °C), (2) the onset temperature, 160 °C for transformation from cage to network structure, and (3) the immobilization temperature, 175 °C, which have been described in Fig. 4a–c. Noticeable porogen aggregation occurred at $T > T_g$, but the aggregation occurred at a different rate during these 3 stages, depending on the diffusivity of PS particles, which is a function of viscosity and temperature as described by the Einstein-Stokes equation [34] (Eq. (2)):

$$D = \frac{k_B T}{6\pi\eta r} \tag{2}$$

where $k_B$ is the Boltzmann constant, $T$ is the absolute temperature, $\eta$ is the viscosity of the system and $r$ is the particle radius. In this study, $\eta$, is a measure of the steric and electrostatic barrier to movement of the PS particles within the cross-linkable MSQ matrix. Thus, at $T > T_g$, the relaxation of the PS and MSQ molecular chains leads to reduced viscosity and higher diffusivity of the PS particles. Such high diffusivity increases PS collisions and leads to the aggregation of PS porogens from 10.0 to 13.4 nm. At $T > 160$ °C, the viscosity drops drastically to $\sim 1.8 \times 10^5$ poises, because of the plasticization by the large amount of $H_2O$ by-products when extensive transformation of cage to network Si–O occurs in the MSQ. This results in greater aggregation of the PS porogens, leading to a faster change in the porogen size, from 13.4 to 15.6 nm, between 150 and 175 °C. In the final stage, ~175 to 200 °C, most $H_2O$ is believed to have dried off at less than 175 °C. In addition, the cross-linking of the MSQ matrix with a 3D and highly cross-linked Si–O network structure at $T > 175$ °C makes the MSQ/PS hybrid behave like a solid, with a very high viscosity of $\sim 2.2 \times 10^5$ poises. As a result, the PS porogens are trapped or "frozen" within the highly cross-linked MSQ matrix, leading to an approximately constant porogen size of 15.6–16.5 nm, beyond $T > 175$ °C.

When the surfactant, either anionic or cationic, is added to PS in THF solution, negative or positive charges build up on the PS particle surface. As a result, the charged PS porogens repel each other and do not aggregate. This electrostatic repulsion also plays the dominant role in hindering the aggregation of PS porogens in the NaDBS- and DB-modified PS/MSQ hybrid films during the slow cure process from 30 to 200 °C. Since the surfactant is physically adsorbed only on the PS particle surface, the surface charge on the PS particles may change over time and temperature, if the surfactant desorbs from the surface, during the cure process. However, NaDBS and DB have been reported or tested to possess excellent thermal stability up to at least 200 °C [35]. Therefore, the surface density of NaDBS- or DB-modified PS particles would not be expected to degrade as the cure temperature rises to 200 °C [36,37]. Compared to a weakly electrostatic dispersed PS/MSQ system without modification (zeta potential: −18 mV), the NaDBS-modified PS/MSQ system (zeta potential: −58 mV) and DB-modified PS/MSQ system (zeta potential:+66 mV) exhibits strong electrostatic repulsion, resulting in little or limited aggregation of PS porogens during a slow cure process, which produces a small porogen size with a tight distribution.

The charge on the particles has an effect on the increased viscosity, depending on the surface charge density, because the electrical double layer around each particle is distorted under shearing, *i.e.* the electroviscous effect [38,39]. This increased viscosity can be quantified and taken into account by introducing a correction factor, i.e. the primary electroviscous coeffiicent, $p$, to the modified Einstein-Stokes equation [40] (Eq. (3)):

$$\eta_r = 1 + k(1+p)\varphi \tag{3}$$

where $\eta_r$ is the relative viscosity, $\varphi$ is the volume fraction of the solid and $k = 2.5$ for spherical and rigid particles. The "$p$" coefficient [38] can be represented by Eq. (4)

$$p = \frac{(2\varepsilon_o\varepsilon_r\zeta)^2}{\lambda_o\eta_o a^2} \tag{4}$$

where $\varepsilon_o$ is the permittivity of free space, $\varepsilon_r$ is the relative permittivity, $\zeta$ is the zeta potential, $\lambda_o$ is the specific conductivity of the continuous phase, $\eta_o$ is its viscosity and $a$ is the diameter.

A higher zeta potential leads to a higher viscosity, which accounts for the difference in viscosity among the three different MSQ/PS hybrid films as illustrated in Fig. 4a at $T > T_g$. As a result, the diffusivity of the highly-charged PS porogens is hindered by the increased viscosity. Therefore, the high zeta potential of charged PS porogens further impedes the segregation and aggregation of PS within a successively cross-linked MSQ matrix through electrostatic repulsive forces and the electroviscous effect. In addition, the columbic attraction [30] between the electron lone pair of the oxygen atoms of the Si−OH group and the positively charged PS particles, restrains the PS porogen and its mobility during the cure step, resulting in a further reduction in porogen aggregation. Overall, the NaDBS modified-PS/MSQ hybrid film yielded a small porogen size and tight distribution (8.7 ± 2 nm) when cured at a slow rate up to 200 °C with MSQ fully cross-linked, and a similarly small pore size (8.8 nm) after burning out of porogen at 400 °C. In comparison, our previous work on low-$k$ MSQ/SBS hybrid film used a rapid curing method to trap the porogen within a rapidly formed, well-cross-linked MSQ matrix, leaving its size unchanged (from as-prepared, 25 °C) with tight distribution. Thus, surface modification of PS porogens by cationic surfactant offers an alternative and simple method to control the porogen and pore size and distribution even at a slow cure rate (2 °C/min), which offers great process latitude. This simple method based on polystyrene porogen with surface potential modification, can be further improved by reducing the pore size and extended to other relevant materials as the porogen. In principle, the porogen particle size in the solvent can be reduced by using a porogen of a lower molecular weight [41] and with treatment leading to a higher surface potential [42,43]. As a result, a smaller pore size can be expected after the removal of porogen from the corresponding low-$k$/porogen hybrid film. In addition to polystyrene, the porogen materials can be selected from linear polymers such as polyethylene, polypropylene, poly(-methyl methacrylate) [44], poly(alkylene ether)s (e.g., poly(ethylene oxide) (PEO) and poly(propylene oxide) (PPO)) [45] of lower molecular weight and good miscibility with low-$k$ matrix precursors, such as MSQ.

## 4. Conclusion

A commercial, spin-on MSQ was selected as the low-$k$ matrix and a high-temperature porogen, such as PS, was employed as the sacrificial component in a novel post-integration porogen removal method for preparing porous low-$k$ MSQ film in this paper. The effect of surfactant modification of PS on the porogen size in low-$k$ MSQ/PS hybrid films at 10 wt% PS loading under a slow curing profile was studied by GISAXS, viscosity measurement, and Fourier transform infrared analysis. Specifically, an anionic surfactant, NaDBS, and a cationic surfactant, DB, were used to modify the surface potential of PS porogen in THF solution from an initial value of −18 mV (unmodified) to −58 mV and +66 mV, respectively. Upon curing at a slow rate (2 °C/min), the porogen without modification aggregates and its size increases from 10.0 to 16.5 nm at different rates due to the steric hindrance of the structural state of the MSQ matrix at three particular temperatures; namely, (1) the glass transition temperature, $T_g$ (∼100 °C), (2) the onset temperature (160 °C) for MSQ condensation and (3) the immobilization temperature, 175 °C. The porogen size starts to increase as PS porogen aggregates, at $T > T_g$ of MSQ, then increases at a higher rate, at $T$ between 150 and 175 °C, where the viscosity drops drastically at $T > 160$ °C, and finally increases to 16.5 nm after 190 °C. In contrast, for the NaDBS-modified and DB-modified PS systems, the high zeta potential of charged PS porogens impede the aggregation of PS within a successively cross-linked MSQ matrix through electrostatic repulsion forces and the electroviscous effect. This results in little or limited PS porogen aggregation and yields a small porogen size with tight distribution, 11.1 ± 2.4 and 8.7 ± 2.0 nm, respectively. More importantly, the columbic attraction between the Si−OH groups of MSQ matrix and the DB-modified, positively charged PS particles, restrains the PS porogen and its mobility during the cure step, resulting in a further reduction in porogen aggregation. Overall, the NaDBS modified-PS/MSQ hybrid film yields a small porogen size and tight distribution (8.7 ± 2 nm) when cured at a slow rate up to 200 °C with MSQ fully cross-linked, and a similarly small pore size (8.8 nm) after burning out of porogen at 400 °C. In summary, we provide an alternative and simple method to control the porogen, pore size and distribution even at a slow cure rate (2 °C/min), offering great process latitude.

## Acknowledgements

The authors would like to thank Kuo-Yuan Hsu for the viscosity rheometer test and Dr. U-Ser Jeng, Dr. Chiu-Hun Su, and Ms. Kuei-Fen Liao of NSRRC for their assistance in the GISAXS measurements. This work was financially supported by the National Science Council of Taiwan under Contract: NSC99-2221-E-009-177 and NSC 101-3113-E-007-001-.

## References

[1] M.T. Bohr, Solid State Technol. 9 (1996) 105–111.
[2] Y.H. Wang, R. Kumar, J. Electrochem. Soc. 151 (2004) F73–76.

[3] S.J. Martin, J.P. Godschalx, M.E. Mills, E.O. Shaffer, P.H. Townsend, Adv. Mater. 12 (2000) 1769–1778.
[4] M. Fayolle, G. Passemard, O. Louveau, F. Fusalba, J. Cluzel, Microelectron. Eng. 70 (2003) 255–266.
[5] M. Ree, J. Yoon, K. Heo, J. Mater. Chem. 16 (2005) 685–697.
[6] J.N. Sun, Y. Hu, W.E. Frieze, W. Chen, D.W. Gidley, J. Electrochem. Soc. 150 (2003) F97–101.
[7] T. Frot, W. Volksen, T. Magbitang, D. Miller, S. Purushothaman, M. Lofaro, R. Bruce, G. Dubois, Interconnect Technology Conference and 2011 Materials for Advanced Metallization (IITC/MAM), IEEE International (2011) 1-3.
[8] H. Shi, H. Huang, J. Bao, J. Im, P. S. Ho, Y. Zhou, J. T. Pender, M. Armacost, D. Kyser, Conference Proceedings of the IEEE International Interconnect Technology (IITC) (2009) 78-80.
[9] J. Calvert, M. Gallagher, Semicond. Int. 26 (2003) 56–60.
[10] S. Malhouitre, C. Jehoul, J.V. Aelst, H. Struyf, S. Brongersma, L. Carbonell, I. Vos, G. Beyer, M.V. Hove, D. Gronbeck, M. Gallagher, J. Calvert, K. Maex, Microelectron. Eng. 70 (2003) 302–307.
[11] M.-L. Che, C.-Y. Huang, S. Choang, Y.-H. Chen, J. Leu, J. Mater. Res. 25 (2010) 1049–1056.
[12] K.H. Lee, J.-H. Yim, M.R. Baklanov, Microporous Mesoporous Mater. 94 (2006) 113–121.
[13] Y.-H. Chen, U.-S. Jeng, J. Leu, J. Electrochem. Soc. 158 (2011) G52–57.
[14] A. Zenasni, F. Ciaramella, V. Jousseaume, Ch. Le Cornec, G. Passemard, J. Electrochem. Soc. 154 (2007) G6–12.
[15] W. Oh, T.J. Shin, M. Ree, M.Y. Jin, K. Char, Mol. Cryst. Liq. Cryst. Sci. Technol. Sect. A 371 (2001) 397–402.
[16] T.C. Hodge, B. Landmann, S.A. Bidstrup, P.A. Kohl, Int. J. Microcircuits Electron. Packag. 17 (1994) 10–20.
[17] J. Hang, L. Shi, X. Feng, L. Xiao, Powder Technol. 192 (2009) 166–170.
[18] B.V. Derjaguin, S.S. Dukhin, A.E. Yaroshchuk, J. Colloid Interface Sci. 115 (1987) 234–239.
[19] A.B. Jódar-Reyes, J.L. Ortega-Vinuesa, A. Martín-Rodríguez, J. Colloid Interface Sci. 297 (2006) 170–181.
[20] J.-F. Lee, M.-H. Hsu, H.-P. Chao, H.-C. Huang, S.-P. Wang, J. Hazard. Mater. 114 (2004) 123–130.
[21] R.J. Roe, Methods of X-ray and Neutron Scattering in Polymer Science, Oxford University Press, New York, 2000.
[22] A. Guinier, G. Fournet, Small-Angle Scattering of X-rays, John Wiley & Sons, New York, 1955.
[23] T. Cosgrove, Colloid Science: Principles, Methods and Applications, John Wiley & Sons, New York, 2010.
[24] A. Drechsler, K. Grundke, Colloids Surf., A 264 (2005) 157–165.
[25] P.F. Luckham, Adv. Colloid Interface Sci. 111 (2004) 29–47.
[26] W. Li, P. Chen, M. Gu, Y. Jin, J. Eur. Ceram. Soc. 24 (2004) 3679–3684.
[27] W.C. Liu, C.C. Yang, W.C. Chen, B.T. Dai, M.S. Tsai, J. Non-Cryst. Solids 311 (2002) 233–240.
[28] B. Xie, A.J. Muscat, Microelectron. Eng. 76 (2004) 52–59.
[29] C.D. Volpe, S. Dirè, E. Pagani, J. Non-cryst. Solids 209 (1997) 51–60.
[30] M.A.M. Khraisheh, M.A. Al-Ghouti, S.J. Allen, M.N. Ahmad, Water Res. 39 (2005) 922–932.
[31] P.F. Mcmillan, R.L. Remmele Jr., Am. Mineral. 71 (1986) 772–778.
[32] H.W. Ro, E.S. Park, C.L. Soles, D.Y. Yoon, Chem. Mater. 22 (2010) 1330–1339.
[33] S.S. Dukhin, A.E. Yaroshchuk, B.V. Deryagin, Colloid J. USSR 46 (1984) 191–196.
[34] T. Halpin-Healy, Y.-C. Zhang, Phys. Rep. 254 (1995) 215–414.
[35] A. Uygun, O. Turkoglu, S. Sen, E. Ersoy, A.G. Yavuz, G.G. Batir, Curr. Appl. Phys. 9 (2009) 866–871.
[36] D. Duracher, F. Sauzedde, A. Elaissari, C. Pichot, L. Nabzar, Colloid Polym. Sci. 276 (1998) 920–929.
[37] R. Pelton, D. Zhang, K.L. Thompson, S.P. Armes, Langmuir 27 (2011) 2118–2123.
[38] M.J. Garcia-Salinas, F.J. de las Nieves, Colloid Surf. A: Phys. Eng. 222 (2003) 65–77.
[39] G. Navaneetham, J.D. Posner, J. Fluid Mech. 619 (2009) 331–365.
[40] P.C. Hiemenz, R. Rajagopalan, Principles of Colloid and Surface Chemistry, Marcel Dekker, New York, 1997. pp. 145.
[41] Y. Liu, S. Bo, Y. Zhu, W. Zhang, Polymer 44 (2003) 7209–7220.
[42] K. Kandori, H. Ishiguro, K. Kon-no, A. Kitahara, Langmuir 5 (1989) 1258–1261.
[43] H. Kishimoto, M. Watanabe, T. Iyoda, K. Nagai, M. Nakagawa, Chem. Lett. 35 (2006) 598–599.
[44] T.R. Aslamazova, K. Tauer, Colloid Surf. A-Physicochem. Eng. Asp. 300 (2007) 260–267.
[45] M.P. Ryder, K.F. Schilke, J.A. Auxier, J. McGuire, J.A. Neff, J. Colloid Interface Sci. 350 (2010) 194–199.